Annals of Biomedical Engineering, Vol. 27, pp. 607–616, 1999
Printed in the USA. All rights reserved.

0090-6964/99/27(5)/607/10/$15.00

Generalized Sensitivity Functions in Physiological System Identification

KARL THOMASETH and CLAUDIO COBELLI

Institute of Systems Science and Biomedical Engineering, (LADSEB–CNR), Padova, Italy and Department of Electronics and Informatics, University of Padova, Padova, Italy

(Received 7 August 1998; accepted 12 July 1999)

Abstract—Parameters of physiological models are commonly associated in an input–output experiment with a specific pattern of the system response. This association is often made on an intuitive basis by traditional sensitivity analysis, i.e., by inspecting the variations of model output trajectories with respect to parameter variations. However, this approach provides limited information since, for instance, it ignores correlation among parameters. The aim of this study is to propose a new set of sensitivity functions, called the generalized sensitivity functions (GSF), for the analysis of input–output identification experiments. GSF are based on information theoretical criteria and provide, as compared to traditional sensitivity analysis, a more accurate picture on the information content of measured outputs on individual model parameters at different times. Case studies are presented on an input–output model and on two structural circulatory and respiratory models. GSF allow the definition of relevant time intervals for the identification of specific parameters and improve the understanding of the role played by specific model parameters in describing experimental data. © *1999 Biomedical Engineering Society.*
[S0090-6964(99)00605-0]

Keywords—Experiment design, Parameter estimation, Circulatory model, Respiratory model.

INTRODUCTION

The parameters of a structural model of a physiological system are commonly associated in an input–output experiment with specific patterns of the system response. In fact, often the observation interval is divided into subintervals each of which is presumed to be informative on a specific parameter. Knowledge of these subintervals is not only important for understanding the role of model parameters, but also for an enhanced experiment design for estimating selected parameters. The above knowledge is typically gathered through an intuitive reasoning based on traditional sensitivity analysis, i.e., the quantification of the effects of variations in model parameters on the time courses of model outputs. This approach, while useful in simulation studies for assessing the sensitivity of the output with respect to assigned model parameters, is of limited utility in system identification studies where model parameters are estimated from noisy experimental data and correlation among parameter estimates is present.

Our aim is to introduce a new set of sensitivity functions, called generalized sensitivity functions (GSF), for the analysis of system identification experiments. GSF work in a parameter estimation context and allow one to assess qualitatively where the information on specific parameters is concentrated during an identification experiment. GSF will be introduced within a weighted least-squares (WLS) parameter estimation context assuming, for simplicity, a frequently sampled measured output, such as that available in studies which virtually allow a continuous-time monitoring of a physiological system.

THEORY

Models of physiological systems are represented for notational simplicity as nonlinear regression functions $f(t,\boldsymbol{\theta})$ with time t as independent variable and with parameter vector $\boldsymbol{\theta}$. We consider single-output models with discrete-time noisy measurements given as

$$y(t_k)=f(t_k,\boldsymbol{\theta})+e(t_k), \quad k=1,\ldots,M, \tag{1}$$

where $e(t_k)$ is the measurement noise assumed to be independently and identically distributed with zero mean and known, possibly time-varying, variance $\sigma^2(t_k)$ which is independent of model parameters. Nominal values of parameters and of other variables, e.g., model inputs or sampling schedule, are assumed to be known.

Traditional Sensitivity Functions

Traditional sensitivity analysis is performed by visual inspection of the time courses of the derivatives of $f(t,\boldsymbol{\theta})$ with respect to the parameters, in vector notation

Address correspondence to: Karl Thomaseth, PhD, LADSEB–CNR, Corso Stati Uniti 4, 35127 Padova, Italy. Electronic mail: Karl.Thomaseth@ladseb.pd.cnr.it

$\nabla_{\boldsymbol{\theta}} f(t,\boldsymbol{\theta})$.[7] These functions represent the changes in model output trajectories with respect to small variations in model parameters according to

$$\delta y(t_k) = \nabla_{\boldsymbol{\theta}} f(t_k,\boldsymbol{\theta})' \,\delta\boldsymbol{\theta}. \tag{2}$$

In order to allow a direct comparison of the derivatives between different parameters the following vector valued function is introduced which will be referred to as *(normalized) model sensitivities*

$$\mathbf{s}(t) = \mathbf{D}\nabla_{\boldsymbol{\theta}} f(t,\boldsymbol{\theta}). \tag{3}$$

The elements of the diagonal scaling matrix $\mathbf{D}$ are calculated with reference to the sampling schedule as

$$\mathbf{D} = \operatorname{diag}\left(\sum_{i=1}^{M} \nabla_{\boldsymbol{\theta}} f(t_i,\boldsymbol{\theta}) \bullet \nabla_{\boldsymbol{\theta}} f(t_i,\boldsymbol{\theta}) \right)^{-1/2}, \tag{4}$$

where ''•'' represents element-by-element multiplication.

Generalized Sensitivity Functions

Fundamentals. Traditional sensitivity analysis is appropriate and useful in simulation studies where there is the need to assess the effect of model parameter variations on the time course of model outputs. In contrast with simulation, in identification studies one has a vector of parameter estimates whose components are correlated. To answer the question at which time points measurements are most informative for the estimation of specific parameters, traditional model sensitivities are not well suited because they quantify how model parameter variations would change the model output without taking into account how these model output variations would affect parameter estimates.[12] To overcome this shortcoming we introduce the GSF which can be evaluated as a by-product of a parameter estimation procedure. An important difference with respect to traditional sensitivities is that GSF require *a priori* unique, or at least nonunique, local identifiability of model parameters,[1] i.e., GSF cannot be applied to all the parameters of a nonidentifiable model but only to the subset of identifiable ones.

It is assumed, for simplicity, that the observations $y(t_k)$ are obtained from Eq. (1) with a *true* parameter vector $\boldsymbol{\theta}_0$ which is estimated in the time domain with nonlinear WLS, i.e., by minimizing the weighted residual sum of squares (WRSS):

$$\mathrm{WRSS}(\mathbf{y},\boldsymbol{\theta}) = \sum_{i=1}^{M} \frac{[y(t_i) - f(t_i,\boldsymbol{\theta})]^2}{\sigma^2(t_i)}, \tag{5}$$

where $\mathbf{y} = [y(t_1), \ldots, y(t_M)]'$ represents the column vector of observations. WLS parameter estimation is also adequate if the measurement noise variance is only known up to a scale factor, which can be estimated from the final WRSS.[8]

WLS estimates are defined as

$$\hat{\boldsymbol{\theta}} = \arg\min_{\boldsymbol{\theta}} \mathrm{WRSS}(\mathbf{y},\boldsymbol{\theta}), \tag{6}$$

and must satisfy the optimality condition

$$\begin{aligned} \nabla_{\boldsymbol{\theta}} \mathrm{WRSS}(\mathbf{y},\boldsymbol{\theta})\big|_{\boldsymbol{\theta}=\hat{\boldsymbol{\theta}}} &= -2\sum_{i=1}^{M} \frac{(y(t_i) - f(t_i,\hat{\boldsymbol{\theta}}))}{\sigma^2(t_i)} \nabla_{\boldsymbol{\theta}} f(t_i,\hat{\boldsymbol{\theta}}) \\ &\equiv \nabla_{\boldsymbol{\theta}} \mathrm{WRSS}(\mathbf{y},\hat{\boldsymbol{\theta}}) = \mathbf{0}. \end{aligned} \tag{7}$$

It is assumed that parameter estimates are unbiased, i.e., that $\mathrm{E}[\hat{\boldsymbol{\theta}}] = \boldsymbol{\theta}_0$. By considering a small perturbation $\delta\boldsymbol{\theta}_0$ of the *true* parameters, the model output varies according to Eq. (2), and we define

$$\delta\mathbf{y} = \begin{bmatrix} \nabla_{\boldsymbol{\theta}} f(t_1,\boldsymbol{\theta}_0)' \\ \vdots \\ \nabla_{\boldsymbol{\theta}} f(t_M,\boldsymbol{\theta}_0)' \end{bmatrix} \delta\boldsymbol{\theta}_0. \tag{8}$$

This output variation, assumed independent of measurement error, causes a variation $\delta\hat{\boldsymbol{\theta}}$ of the parameter estimates such that Eq. (7) still holds, i.e.,

$$\begin{aligned} \mathbf{0} &= \nabla_{\boldsymbol{\theta}} \mathrm{WRSS}(\mathbf{y} + \delta\mathbf{y}, \hat{\boldsymbol{\theta}} + \delta\hat{\boldsymbol{\theta}}) \\ &\approx \nabla^2_{\boldsymbol{\theta}^2} \mathrm{WRSS}(\mathbf{y},\hat{\boldsymbol{\theta}})\,\delta\hat{\boldsymbol{\theta}} + \nabla^2_{\boldsymbol{\theta}\mathbf{y}} \mathrm{WRSS}(\mathbf{y},\hat{\boldsymbol{\theta}})\,\delta\mathbf{y}, \end{aligned} \tag{9}$$

where $\nabla^2_{\boldsymbol{\theta}^2}$ and $\nabla^2_{\boldsymbol{\theta}\mathbf{y}}$ represent second-order derivatives.

Equation (9) yields the approximation

$$\delta\hat{\boldsymbol{\theta}} \approx -[\nabla^2_{\boldsymbol{\theta}^2} \mathrm{WRSS}(\mathbf{y},\hat{\boldsymbol{\theta}})]^{-1} \nabla^2_{\boldsymbol{\theta}\mathbf{y}} \mathrm{WRSS}(\mathbf{y},\hat{\boldsymbol{\theta}})\,\delta\mathbf{y}, \tag{10}$$

which will be combined with Eq. (8).

From Eq. (7) one has

$$\begin{aligned} \nabla^2_{\boldsymbol{\theta}^2} \mathrm{WRSS}(\mathbf{y},\boldsymbol{\theta}) = 2\Bigg[&\sum_{i=1}^{M} \frac{1}{\sigma^2(t_i)} \nabla_{\boldsymbol{\theta}} f(t_i,\boldsymbol{\theta}) \nabla_{\boldsymbol{\theta}} f(t_i,\boldsymbol{\theta})' \\ &- \sum_{i=1}^{M} \frac{(y(t_i) - f(t_i,\boldsymbol{\theta}))}{\sigma^2(t_i)} \nabla^2_{\boldsymbol{\theta}^2} f(t_i,\boldsymbol{\theta}) \Bigg], \end{aligned} \tag{11}$$

$$\frac{d\nabla_{\boldsymbol{\theta}}\mathrm{WRSS}(\mathbf{y},\boldsymbol{\theta})}{dy(t_i)} = -\frac{2}{\sigma^2(t_i)}\nabla_{\boldsymbol{\theta}} f(t_i,\boldsymbol{\theta}). \tag{12}$$

In order to derive equations that do not depend explicitly on the data we consider the *a priori* expected values of the matrices in Eq. (10). In particular, from Eqs. (11) and (12) we obtain

$$\mathrm{E}[\nabla^2_{\boldsymbol{\theta}^2}\mathrm{WRSS}(\mathbf{y},\hat{\boldsymbol{\theta}})|_{\hat{\boldsymbol{\theta}}=\boldsymbol{\theta}_0}] = 2\sum_{i=1}^{M}\frac{1}{\sigma^2(t_i)}\nabla_{\boldsymbol{\theta}} f(t_i,\boldsymbol{\theta}_0)\nabla_{\boldsymbol{\theta}} f(t_i,\boldsymbol{\theta}_0)', \tag{13}$$

$$\mathrm{E}[\nabla^2_{\boldsymbol{\theta}\mathbf{y}}\mathrm{WRSS}(\mathbf{y},\hat{\boldsymbol{\theta}})|_{\hat{\boldsymbol{\theta}}=\boldsymbol{\theta}_0}] = -2\left[\frac{\nabla_{\boldsymbol{\theta}} f(t_1,\boldsymbol{\theta}_0)}{\sigma^2(t_1)},\ldots,\frac{\nabla_{\boldsymbol{\theta}} f(t_M,\boldsymbol{\theta}_0)}{\sigma^2(t_M)}\right]. \tag{14}$$

By replacing Eqs. (13) and (14) in Eq. (10), we obtain

$$\delta\hat{\boldsymbol{\theta}} \approx \left[\sum_{j=1}^{M}\frac{1}{\sigma^2(t_j)}\nabla_{\boldsymbol{\theta}} f(t_j,\boldsymbol{\theta}_0)\nabla_{\boldsymbol{\theta}} f(t_j,\boldsymbol{\theta}_0)'\right]^{-1} \times\sum_{i=1}^{M}\frac{\nabla_{\boldsymbol{\theta}} f(t_i,\boldsymbol{\theta}_0)}{\sigma^2(t_i)}\delta y(t_i), \tag{15}$$

and by taking into account Eq. (2), Eq. (15) becomes

$$\delta\hat{\boldsymbol{\theta}} \approx \left(\left[\sum_{j=1}^{M}\frac{1}{\sigma^2(t_j)}\nabla_{\boldsymbol{\theta}} f(t_j,\boldsymbol{\theta}_0)\nabla_{\boldsymbol{\theta}} f(t_j,\boldsymbol{\theta}_0)'\right]^{-1} \times\sum_{i=1}^{M}\frac{\nabla_{\boldsymbol{\theta}} f(t_i,\boldsymbol{\theta}_0)}{\sigma^2(t_i)}\nabla_{\boldsymbol{\theta}} f(t_i,\boldsymbol{\theta}_0)'\right)\delta\boldsymbol{\theta}_0 = \mathbf{I}\delta\boldsymbol{\theta}_0, \tag{16}$$

where $\mathbf{I}$ is the identity matrix. Equation (16) satisfies the hypothesis that parameter estimates are unbiased, i.e., the variation $\delta\hat{\boldsymbol{\theta}}$ of the parameter estimates is equal to the variation $\delta\boldsymbol{\theta}_0$ of the true model parameters. Moreover, Eq. (16) indicates that variations of the true parameter values are estimated independently from each other because the off-diagonal elements of the matrix operation in Eq. (16) are equal to zero. For this reason, we will consider in the following only the elements on the main diagonal of the matrix in Eq. (16).

Definition. Equation (16) has been obtained as the combination of the sensitivities of parameter estimates with respect to changes in model outputs, Eq. (10), and of the sensitivities of model outputs with respect to model parameters, Eq. (2). This motivates the introduction of GSF defined at the time points $\{t_k, k=1,\ldots,M\}$, $\mathbf{gs}(t_k)$, that show how the effect of variations in the true parameters on their estimates distributes during the experiment

$$\mathbf{gs}(t_k) = \sum_{i=1}^{k}\left\{\left(\left[\sum_{j=1}^{M}\frac{1}{\sigma^2(t_j)}\nabla_{\boldsymbol{\theta}} f(t_j,\boldsymbol{\theta}_0)\nabla_{\boldsymbol{\theta}} f(t_j,\boldsymbol{\theta}_0)'\right]^{-1} \times\frac{\nabla_{\boldsymbol{\theta}} f(t_i,\boldsymbol{\theta}_0)}{\sigma^2(t_i)}\right)\bullet\nabla_{\boldsymbol{\theta}} f(t_i,\boldsymbol{\theta}_0)\right\}. \tag{17}$$

GSF of Eq. (17) have been derived from Eq. (16) by taking into account only the contribution of the first k measurements [right-hand-side summation in Eq. (15) or (16)], and by describing only the diagonal elements of the matrix in Eq. (16) through the element-by-element multiplication "$\bullet$". From the identity relationship of Eq. (16) it follows that GSF have a unit value at the end of the experiment, i.e., $\mathbf{gs}(t_M)=\mathbf{1}$, where $\mathbf{1}$ is the unit vector. If we consider $\mathbf{gs}(t)=\mathbf{0}$ for $t<t_1$, i.e., before the first observation is collected, then there is a transition of GSF from 0 to 1 during the experiment. According to the interpretation given to Eq. (17), the time interval during which this transition occurs for a particular component of $\mathbf{gs}(t_k)$ can be viewed as the time interval during which data provide most information on possible variations in the corresponding true model parameter. The actual information is associated with the rate of change of GSF (see the appendix), and thus sharp increases of GSF indicate a high concentration of information about parameters. As shown in the examples, the transition from 0 to 1 is not necessarily monotonically increasing, but can be accompanied by oscillations that will be present if large correlations between parameter estimates exist. This can be explained by observing that GSF of Eq. (17) are obtained from the covariance matrix of parameter estimates (see the appendix) and from the traditional sensitivity functions. It is easy to show that GSF are monotonically nondecreasing if the covariance matrix is diagonal, i.e., if parameter estimates are uncorrelated. However, this is only a sufficient but not a necessary condition. Only the sum of all components of $\mathbf{gs}(t_k)$ is nondecreasing, i.e., $\mathbf{gs}(t_{k+1})'\mathbf{1} \geqslant \mathbf{gs}(t_k)'\mathbf{1}$. This property follows from the interpretation given to GSF within an information theoretical framework, as discussed in the appendix.

(1) **Remark 1:** It can be noted that Eq. (10) defines sensitivities of parameter estimates with respect to model outputs and is generally applicable to parameter estimation problems formulated according to Eq. (6). In particular, the weighted residual sum of squares WRSS of Eq. (5) can be replaced by other objective functions such as the negative log likeli-

hood used in maximum likelihood or Bayesian parameter estimation. Moreover, the validity of Eq. (10) is not restricted to measured outputs and is applicable, after suitable substitution of **y**, for determining variations of parameter estimates with respect to variations of other assigned model variables, e.g., inputs or constants.[11]

(2) **Remark 2:** It should be noted that the linearization Eq. (10) is valid in a neighborhood of the optimal solution, Eq. (6), and can be used in an *a posteriori* analysis by computing the exact second-order derivatives according to Eqs. (11) and (12) with $\boldsymbol{\theta}$ replaced by $\hat{\boldsymbol{\theta}}$. Thus, second-order derivatives can be calculated numerically and this makes the approach generally applicable even if the cost function used for estimation is not WRSS, Eq. (5), or if the approximations Eqs. (13) and (14) are poor, e.g., due to high estimation residuals.[8]

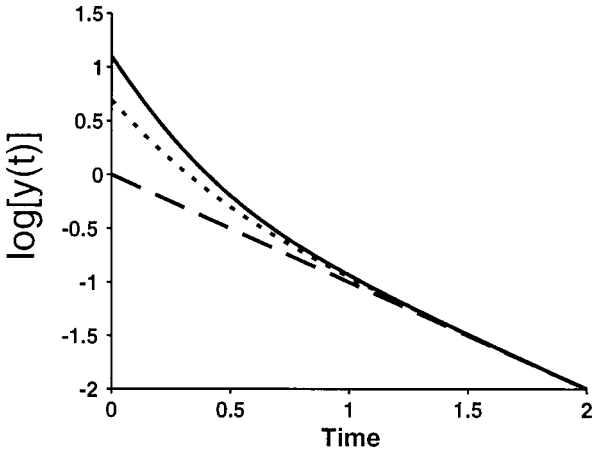

FIGURE 1. Logarithmic representation of the three-exponential function of Eq. (18) (continuous line); two-exponential approximation by the two slowest components, i.e., $y(t) \approx e^{-\alpha_2 t} + e^{-\alpha_3 t}$ (dotted line); and one-exponential approximation by the slowest component, i.e., $y(t) \approx e^{-\alpha_3 t}$ (dashed line).

EXAMPLES

The theory is exemplified first on an input–output three-exponential model and subsequently on two published dynamic structural models of physiological systems, i.e., a three-element Windkessel model of aortic impedance[4,13] and a four element model of respiratory mechanics.[2] The case studies serve as a test-bed for the theory. In the two circulatory and respiratory examples the time course of blood flow and air flow are viewed, respectively, as forcing inputs while blood pressure and air pressure are the model outputs. Both models can be represented by an electrical analog. According to conventional notations elastic elements (capacitors) are characterized either by their compliance or their inverse elastance. The models are defined in terms of state equations with volumes as state variables with initial conditions parametrized as initial pressure times compliance (or divided by elastance). The estimated parameters $\boldsymbol{\theta}$ also include the initial pressures across the elastic elements. Differential model equations and their sensitivities with respect to model parameters were generated symbolically using the software tool PANSYM.[9] Numerical integration was performed using a variable stepsize fourth-order Runge Kutta method. Parameter estimation was carried out in the programming environment MATLAB™ using a previously developed software.[10]

An Input–Output Model

We consider an input–output three-exponential model described by

$$y(t) = e^{-\alpha_1 t} + e^{-\alpha_2 t} + e^{-\alpha_3 t} + e(t), \qquad (18)$$

where $e(t)$ is assumed to be zero mean white noise with constant unit variance. Nominal values for the estimated parameters are chosen equal to $\alpha_1 = 5$, $\alpha_2 = 4$, and $\alpha_3 = 1$ to obtain two fast and one slow exponential components. The sensitivity analysis was carried out for an observation interval $0 \leqslant t \leqslant 2$, with sampling interval equal to 0.01. The corresponding logarithmic time course of a noise-free output is shown in Fig. 1 together with the slower one- and two-exponential approximations.

Given the numerical values assigned to $\{\alpha_i, i = 1, \ldots, 3\}$, a strong correlation is expected between the parameters of the two fast exponentials, i.e., α_1 and α_2. In fact one has for the correlation coefficients: $\mathrm{Corr}(\alpha_1, \alpha_2) = -0.986$, $\mathrm{Corr}(\alpha_1, \alpha_3) = 0.644$, and $\mathrm{Corr}(\alpha_2, \alpha_3) = -0.709$.

Traditional and generalized sensitivity functions of $y(t)$, Eq. (18), are shown in Figs. 2(a) and 2(b), respectively. The traditional sensitivity of α_3 is, as expected, delayed with respect to the sensitivities of α_1 and α_2, which are on the other hand close to each other. This latter fact is also the cause of the high correlation between α_1 and α_2. On the contrary, the GSF of Fig. 2(b) show very different time courses during their transition from 0 to 1. In particular, the initial increase of the GSF of α_1 indicates that the information on this parameter is available at the beginning of the observation interval. The correlation between α_1 and α_2 is reflected in an overshoot of the GSF of α_1 and an initial decrease of the GSF of α_2. According to Fig. 2(b), and in agreement with intuitive reasoning, the information on α_2 is obtained from the data in the central part of the observation interval, whereas only the ''end'' data are informative for α_3.

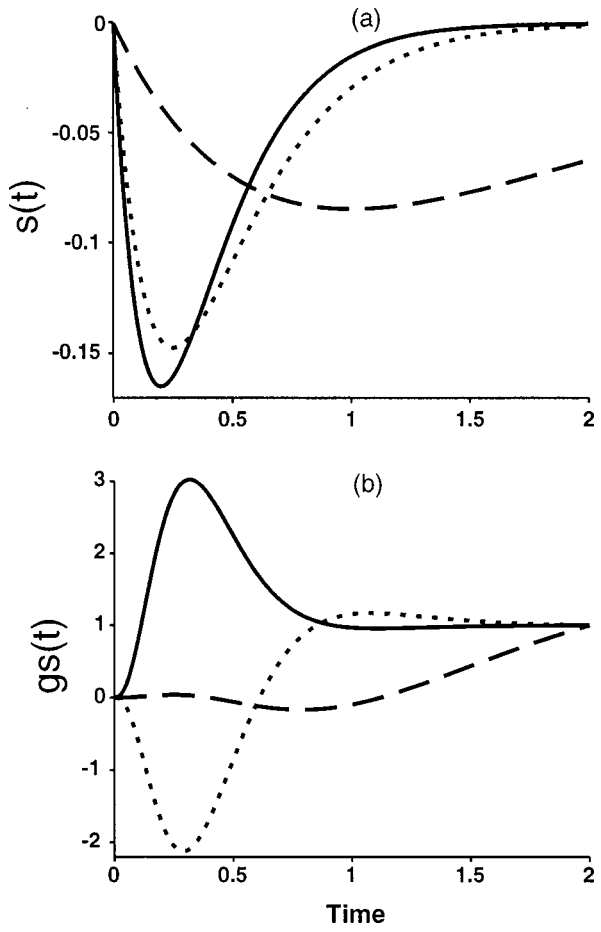

FIGURE 2. Sensitivity analysis of the three-exponential model of Eq. (18) according to (a) normalized model sensitivities, Eq. (3), and (b) generalized sensitivity functions, Eq. (17). Line types represent parameters as follows: continuous α_1; dotted α_2; and dashed α_3.

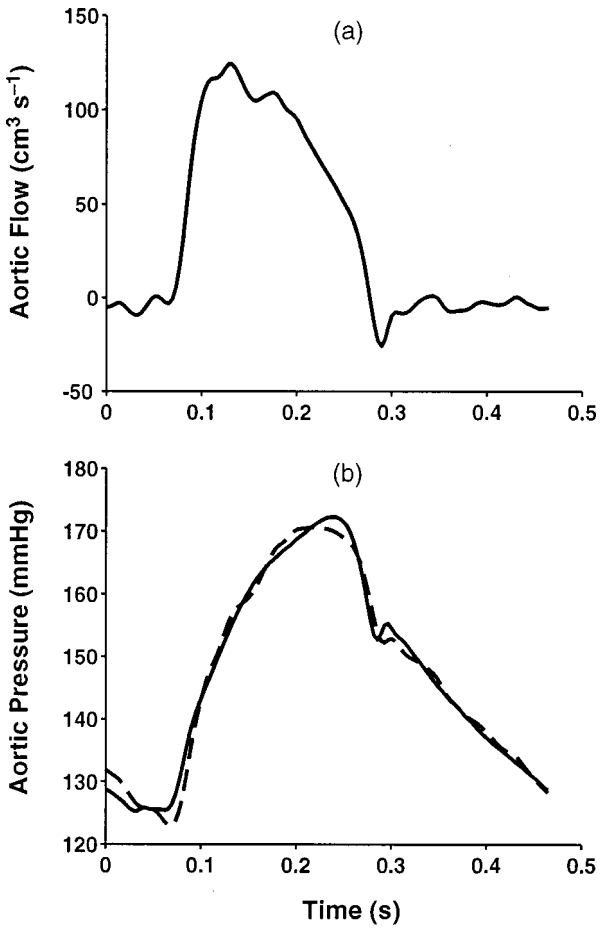

FIGURE 4. (a) Blood flow and [(b) continuous line] pressure measured in the ascending aorta of a dog under vasoconstricted condition, Ref. 3, and [(b) dashed line] model fit.

A Circulatory Model

The three-element Windkessel model used to describe aortic impedance in the dog is shown in Fig. 3 and is described by the following linear dynamic system equations:

$$\dot{x}(t) = -\frac{x(t)}{R_p C} + u(t), \quad x(t_0) = P_0 C, \tag{19}$$

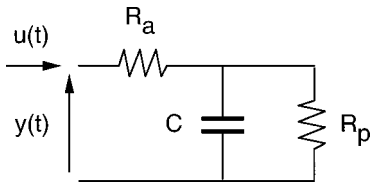

FIGURE 3. Electrical analog of the three-element Windkessel model of aortic impedance.

$$y(t) = \frac{x(t)}{C} + R_a u(t), \tag{20}$$

where $y(t)$ (mm Hg) and $u(t)$ (cm^3 s^{-1}) are aortic blood pressure and flow, respectively; $x(t)$ (cm^3) represents blood volume in the large vessels that are characterized by the compliance C (cm^3 mm Hg^{-1}); R_p (mm Hg s cm^{-3}) is the peripheral resistance of the microcirculation; and R_a (mm Hg s cm^{-3}) quantifies the resistance to flow of the large vessels. The initial condition $x(t_0)$ depends on the initial pressure P_0 which is estimated along with the other parameters, i.e., $\boldsymbol{\theta} = [C, R_a, R_p, P_0]$.

The chosen model structure yields rather simple model equations that help intuitive reasoning in line with the goal of this study.

The time courses of aortic blood flow and pressure together with the model fit are shown in Fig. 4 for a dog experiment under pharmacological vasoconstriction (data are the same as in Ref. 3 and Fig. 5). Data were sampled from pressure and flow transducer signals at 250

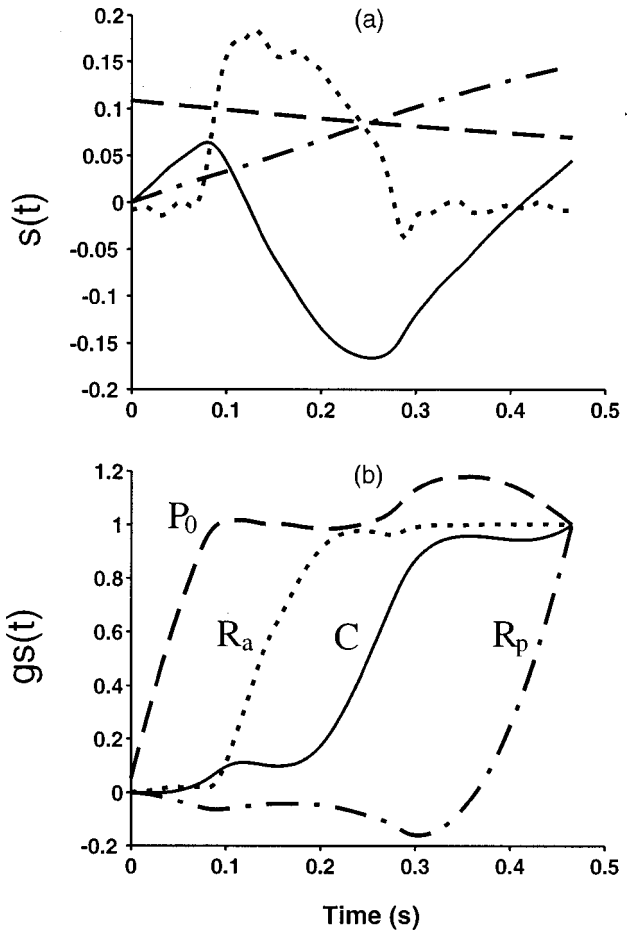

FIGURE 5. Sensitivity analysis of the identification experiment of the circulatory model according to (a) normalized model sensitivities, Eq. (3), and (b) generalized sensitivity functions, Eq. (17). Line types represent parameters as follows: continuous C; dashed P_0; dotted R_a; and dash-dotted R_p.

samples/s. Parameter estimation gave the following point estimates and precision (SD): $\hat{C}=0.260$ (0.006), $\hat{R}_a=0.167$ (0.006), $\hat{R}_p=3.94$ (0.06), and $\hat{P}_0=132.8$ (0.6).

Traditional and generalized sensitivity analyses of the identification experiment are shown in Figs. 5(a) and 5(b), respectively. In particular, Fig. 5(a) shows that the sensitivity of the output with respect to the initial aortic pressure P_0 is maximum at time zero and declines slowly throughout the experiment. A different behavior is shown by peripheral resistance R_p which increases steadily from zero to a maximum value at the end of the experiment. The model sensitivity with respect to the aortic resistance R_a follows, as expected, the aortic flow pattern [see Fig. 4(a)]. Finally, the model sensitivity with respect to the compliance C exhibits a variable pattern with a negative peak between 0.2 and 0.3 s.

It can be observed that the traditional sensitivities, Eq. (3) and Fig. 5(a) do not provide, at variance with GSF, a clear picture regarding the information useful for parameter estimation. In fact, Fig. 5(b) shows that for all estimated parameters there is a marked transition of GSF from the initial (zero) to the final (unit) value that occurs in well-defined time intervals. In particular, the information on the initial aortic pressure P_0 is concentrated at the beginning of the observation interval between 0 and 0.1 s; the information on aortic resistance R_a between 0.1 and 0.2 s during the raising phase of blood flow and pressure (see Fig. 4); the information on the compliance C is associated with the pressure peak and subsequent decay between 0.2 and 0.3 s; and finally information on peripheral resistance R_p is associated with the diastolic phase. Details regarding the *changes* over time in information content of measurements for each single parameter are discussed in the appendix.

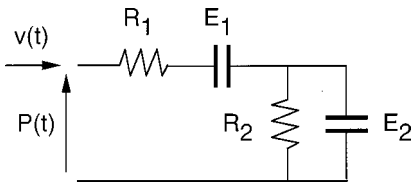

FIGURE 6. Electrical analog of pulmonary impedance during mechanical ventilation.

A Respiratory Model

In the following we consider the two-compartment viscoelastic model of respiratory mechanics proposed by Bates *et al.*[2] The electrical analog of the model is shown in Fig. 6 which gives the following system dynamics and measurement equations:

$$\dot{x}_1(t)=v(t), \quad x_1(t_0)=\frac{P_1(0)}{E_1}, \tag{21}$$

$$\dot{x}_2(t)=v(t)-\frac{E_2}{R_2}x_2(t), \quad x_2(t_0)=\frac{P_2(0)}{E_2}, \tag{22}$$

$$P(t)=E_1x_1(t)+E_2x_2(t)+R_1v(t), \tag{23}$$

where $P(t)$ and $v(t)$ are the measured pulmonary air pressure ($cm\,H_2O$) and airflow ($L\,s^{-1}$), respectively; $x_1(t)$ and $x_2(t)$ represent instantaneous compartmental air volumes (L); E_1 and E_2 are the compartmental elastances ($cm\,H_2O\,L^{-1}$); R_1 and R_2 are resistances ($cm\,H_2O\,s\,L^{-1}$); and $P_1(0)$ and $P_2(0)$ are initial compartmental pressures ($cm\,H_2O$) that are estimated together with the other respiratory mechanical parameters, i.e., $\theta=[E_1,E_2,R_1,R_2,P_1(0),P_2(0)]$.

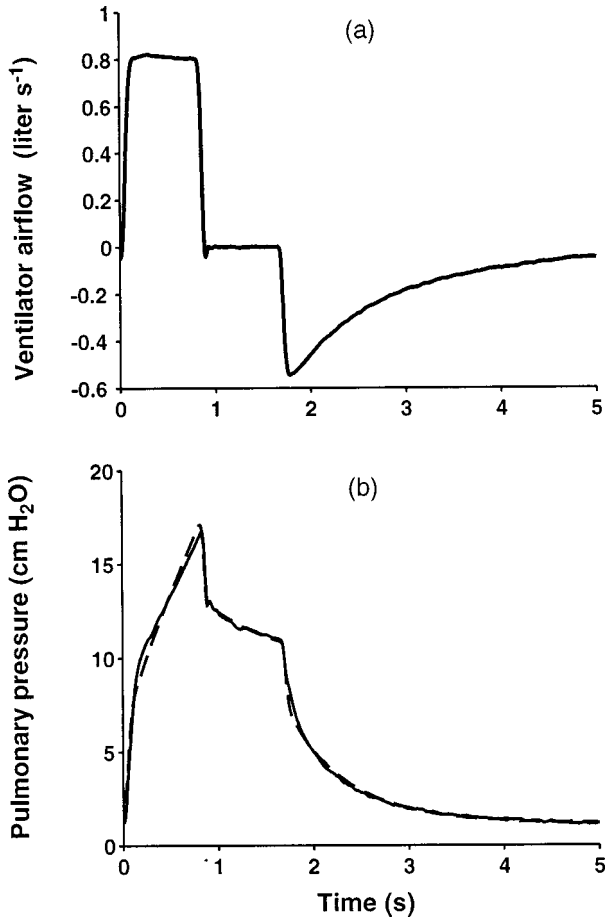

FIGURE 7. (a) Time course of ventilator airflow and [(b) continuous line] pulmonary pressure, determined with correction for dissipative effects of endotracheal tube, together with [(b) dashed line] model predictions.

Experimental data collected in one mechanically ventilated patient are shown in Fig. 7 together with the model fit. In particular, Fig. 7(a) shows the ventilator airflow with step flow forcing and delayed passive expiration, and Fig. 7(b) shows the pulmonary pressure reconstructed from the measured ventilator pressure by compensating for the resistive dissipation in the endotracheal tube. Data were sampled at 100 samples/s.

Parameter estimates and precision (SD) were: $\hat{E}_1 = 11.73$ (0.37), $\hat{E}_2 = 7.94$ (0.20), $\hat{R}_1 = 5.72$ (0.09), $\hat{R}_2 = 6.63$ (0.57), $\hat{P}_1(0) = 2.02$ (0.10), and $\hat{P}_2(0) = 0.65$ (0.15).

The time courses of the traditional sensitivities, Eq. (3), and of GSF, Eq. (17), are shown in Figs. 8(a) and 8(b) and Figs. 8(c) and 8(d), respectively. GSF provide a clear indication on the information content of experimental data for parameters $P_2(0)$, R_1, and E_2 [Fig. 8(c)]. In particular, the estimation of the initial condition $P_2(0)$ is affected only by the early data points [thin dashed line in Fig. 8(c)] in contrast with the corresponding model sensitivity, shown in Fig. 8(a), that decays slowly to zero. The estimate of the resistance R_1 is sensitive mainly to measurements during the first 1 s interval [dotted line in Fig. 8(c)] which corresponds to the forced inspiration [see Fig. 7(a)]. A direct comparison with the model sensitivity [dotted line in Fig. 8(a)] shows that the model output is sensitive to R_1 also during the expiration phase, which provides, however, only little information for the estimation of this parameter. GSF are well defined also for the elastance parameter E_2 [dashed line in Fig. 8(c)], the estimation of which is most affected during the expiration transient between 2 and 3 s. The corresponding model sensitivity [Fig. 8(a)] shows large variations throughout the observation interval.

The interpretation of the sensitivity functions for parameters E_1, R_2, and $P_1(0)$ is more difficult. In particular, traditional sensitivities shown in Fig. 8(b) include a constant value for parameter $P_1(0)$ and similar time courses for parameters E_1 and R_2, respectively. Moreover, GSF shown in Fig. 8(d) exhibit large oscillations for all three parameters with no clear transition from zero to one. This indicates possible *a posteriori* identifiability problems as confirmed by the fact that correlation among these three parameters was: -0.989 between E_1 and R_2; -0.982 between E_1 and $P_1(0)$; and 0.975 between R_2 and $P_1(0)$.

This example shows that GSF provide, in addition to the primary objective of analyzing the measurement information content on parameters, also an indication of possible *a posteriori* identifiability problems for subsets of parameters. Since a general rule for solving identifiability problems is to try first different parametrizations that reduce the number of free adjustable parameters, we illustrate the effects of fixing one parameter to a value very close to the previous estimate, in particular, $P_1(0) = 2.0$. The estimates of the remaining parameters became: $\hat{E}_1 = 11.82$ (0.07), $\hat{E}_2 = 7.93$ (0.19), $\hat{R}_1 = 5.71$ (0.08), $\hat{R}_2 = 6.50$ (0.12), and $\hat{P}_2(0) = 0.68$ (0.08). The corresponding GSF are shown in Fig. 9 which confirms the previous results obtained for parameters E_2, R_1, and $P_2(0)$, and indicates that the information on parameters E_1 and R_2 is available more or less throughout the experiment.

It must be emphasized that the elimination of one estimated parameter $[P_1(0)]$ provides only an apparent advantage, i.e., the correlation between E_1 and R_2 decreases in absolute value to -0.740, but fixing one model parameter to an erroneous value can introduce an estimation bias especially in presence of highly correlated parameters.[11]

CONCLUSIONS

The study of a dynamic physiological model by traditional sensitivity analysis investigates the effects of

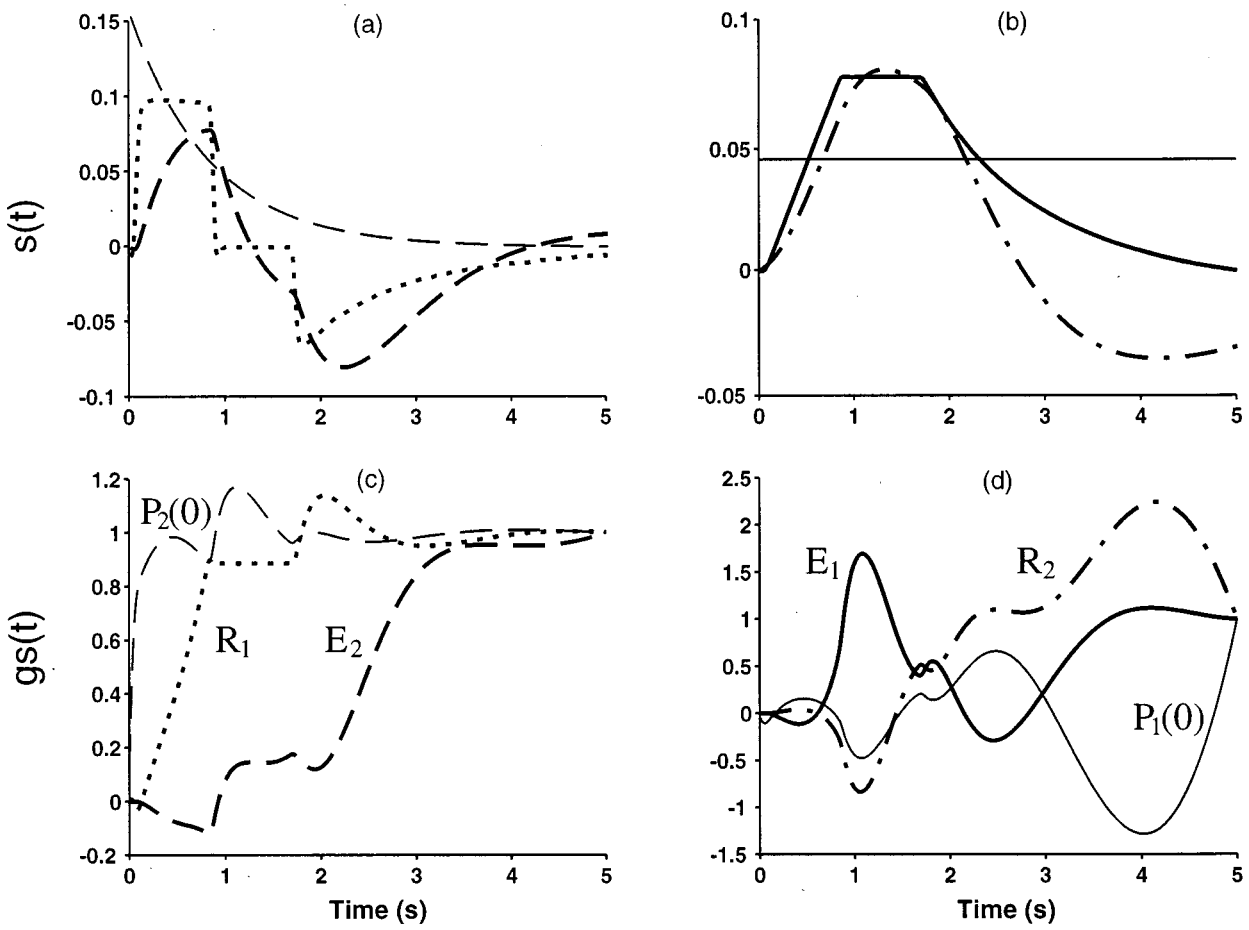

FIGURE 8. Sensitivity analysis of the identification experiment of the respiratory model according to (a) and (b) normalized model sensitivities, Eq. (3), and (c) and (d) GSF, Eq. (17). (a) and (c) correspond to those parameters that show a clear transition from 0 to 1 in GSF; (b) and (d) represent sensitivities for the remaining parameters that exhibit an oscillatory pattern in GSF. Line type/parameter correspondence is: continuous E_1; thin continuous $P_1(0)$; dashed E_2; thin dashed $P_2(0)$; dotted R_1; and dash-dotted R_2.

individual parameter variations on the simulated model output and does not take into account the fact that in a real situation all parameters will be simultaneously estimated from the data and that data are noisy. A new approach to sensitivity analysis has been proposed that combines the sensitivities of the model output with respect to model parameters, Eq. (2), with the sensitivities of parameter estimates with respect to changes in model outputs, Eq. (10). For this reason the proposed GSF of Eq. (17) can be interpreted as the distribution over the experimental observation interval of variations in parameter estimates due to variations in *true* model parameters. Because of unbiasedness, GSF have the interesting property of varying between 0 and 1 from the initial to the final measurement.

The case studies have shown that GSF transition between 0 and 1 occurs frequently during well-defined time intervals. This allows one to divide the experimental interval into subintervals, each of which can be consid-

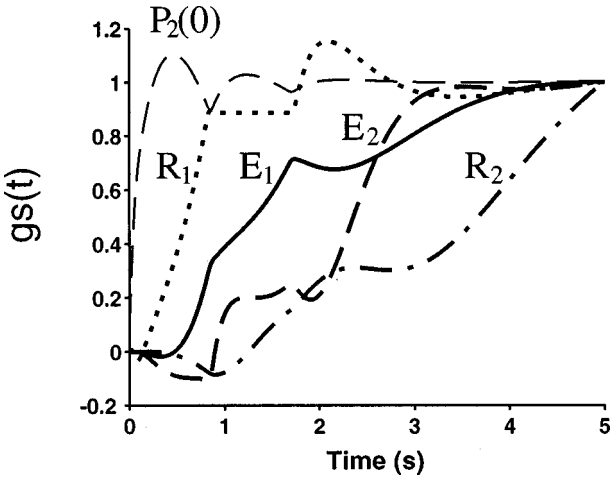

FIGURE 9. GSF, Eq. (17), for the estimation of four respiratory mechanics parameters and only one initial compartmental pressure. Line type/parameter correspondence is: continuous E_1; dashed E_2; thin dashed $P_2(0)$; dotted R_1; and dash-dotted R_2.

ered most informative for a particular parameter. A refined analysis is possible using the incremental GSF, Eq. (A2), as discussed in the appendix, where GSF are considered in an information theoretical framework.

When GSF transition from 0 to 1 is accompanied by large oscillations, numerical identifiability problems for a subset of parameters affected by high correlation are highlighted.

GSF have been derived by considering a WLS parameter estimation context. The basic idea of combining the model output sensitivities, Eq. (2), with the sensitivities of parameter estimates, Eq. (10), is, however, applicable also to different parameter identification approaches. If the simplifying assumptions made in this study are adequate, GSF based on Eqs. (17) and (A2) can be easily obtained as a by-product of any estimation program that provides the covariance matrix of parameter estimates.

ACKNOWLEDGMENTS

The authors wish to thank Professor R. Burattini, Dipartimento di Elettronica e Informatica, Università di Ancona, Italy, and Dr. M. Mergoni, I° Servizio di Anestesia e Rianimazione, Azienda Ospedaliera di Parma, Italy, for kindly providing them with the data of the circulatory and respiratory case studies, respectively.

APPENDIX

We consider in the following the incremental terms of GSF of Eq. (17), denoted with subscript ''inc'' and defined as

$$\mathbf{gs}_{\mathrm{inc}}(t_k)=\mathbf{gs}(t_k)-\mathbf{gs}(t_{k-1}). \tag{A1}$$

According to Eq. (17) we have

$$\mathbf{gs}_{\mathrm{inc}}(t_k)=\left(\left[\sum_{j=1}^{M}\frac{1}{\sigma^2(t_j)}\nabla_{\boldsymbol{\theta}}f(t_j,\boldsymbol{\theta})\nabla_{\boldsymbol{\theta}}f(t_j,\boldsymbol{\theta})'\right]^{-1}\times\frac{\nabla_{\boldsymbol{\theta}}f(t_k,\boldsymbol{\theta})}{\sigma^2(t_k)}\right)\bullet\nabla_{\boldsymbol{\theta}}f(t_k,\boldsymbol{\theta}). \tag{A2}$$

These functions will be referred to as incremental GSF and are closely related to information theoretical criteria as described in the following.

If measurement noise is normal in addition to the previous assumptions the (expected) Fisher information matrix is given as[8]

$$\mathbf{J}(\boldsymbol{\theta})=\sum_{k=1}^{M}\frac{1}{\sigma^2(t_k)}\nabla_{\boldsymbol{\theta}}f(t_k,\boldsymbol{\theta})\nabla_{\boldsymbol{\theta}}f(t_k,\boldsymbol{\theta})'\,\eta_k. \tag{A3}$$

The auxiliary variables $\eta_k=1$ represent unit weights attributed to the measurement $y(t_k)$ taken at time t_k. They are useful to quantify the information on parameters provided by $y(t_k)$ by determining the sensitivity of an information criterion with respect to η_k.[5] In particular, the Fisher information matrix provides an estimate of the inverse of the covariance matrix of parameter estimates, i.e., $\mathbf{Cov}(\hat{\boldsymbol{\theta}})\approx[\mathbf{J}(\hat{\boldsymbol{\theta}})]^{-1}$, and the determinant of the Fisher information matrix, $|\mathbf{J}(\boldsymbol{\theta})|$, or its logarithm are suitable scalar indexes of overall information content on parameters.[6] The information provided by the observation $y(t_k)$ can therefore be quantified as

$$\frac{\partial\log|\mathbf{J}(\boldsymbol{\theta})|}{\partial\eta_k}=\frac{1}{\sigma^2(t_k)}\nabla_{\boldsymbol{\theta}}f(t_k,\boldsymbol{\theta})'[\mathbf{J}(\hat{\boldsymbol{\theta}})]^{-1}\nabla_{\boldsymbol{\theta}}f(t_k,\boldsymbol{\theta})=\mathbf{gs}_{\mathrm{inc}}(t_k)'\mathbf{1}. \tag{A4}$$

Equation (A4) suggests therefore that the elements of $\mathbf{gs}_{\mathrm{inc}}(t_k)$ represent a partition with respect to the model

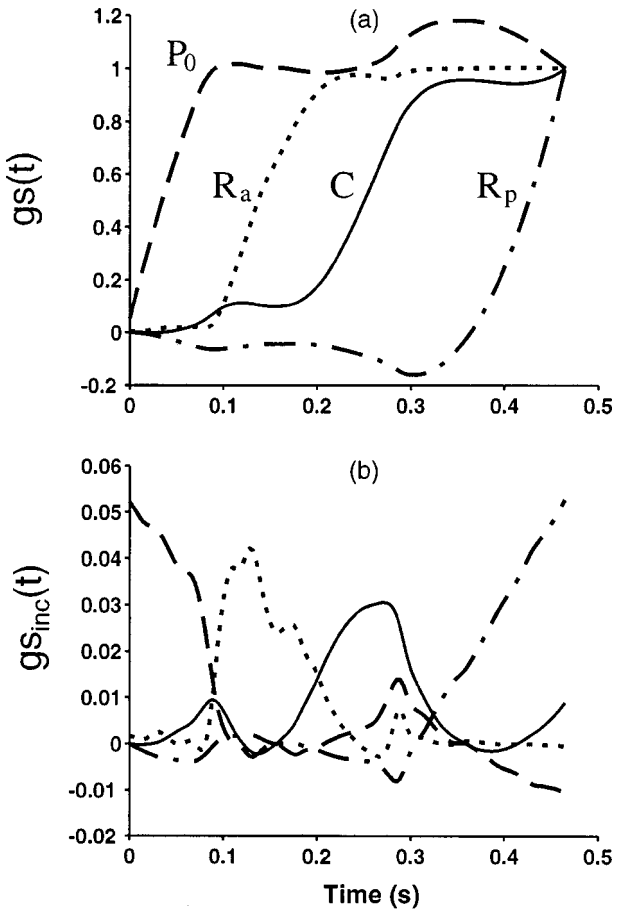

FIGURE A1. Comparison of (a) GSF, Eq. (17), and (b) incremental GSF, Eq. (A2), of the circulatory model. Panel (a) is the same as Fig. 5(b).

parameters of the information provided by the measurement taken at time t_k according to the $\log|\mathbf{J}(\boldsymbol{\theta})|$ criterion. Moreover, the sum of incremental GSF is non-negative because the information matrix is positive definite.

Incremental GSF of Eq. (A2) give therefore a detailed picture of the information provided by single measurements and should be viewed, in addition to their obvious relationship, as a complement to GSF of Eq. (17). The latter are useful for the overall evaluation of the information content of the data by showing where, during the observation interval, the 0–1 transition occurs for each estimated model parameter. The case study on the circulatory model is used for comparing the two approaches (see Fig. A1).

NOMENCLATURE

$f(t, \boldsymbol{\theta})$	nonlinear regression model
$\boldsymbol{\theta}$	vector of estimated parameters
$\hat{\boldsymbol{\theta}}$	parameter estimates
$\boldsymbol{\theta}_0$	nominal model parameters
t_k	sampling time instant
$y(t_k)$	discrete-time measurements
M	total number of samples
WRSS	weighted residual sum of squares
$\mathbf{s}(t)$	normalized model sensitivity
$\mathbf{gs}(t)$	generalized sensitivity function (GSF)
$\mathbf{gs}_{\text{inc}}(t)$	incremental GSF
C	compliance of the large blood vessels
R_p	peripheral blood flow resistance
R_a	aortic blood flow resistance
P_0	initial condition of aortic pressure
$E_{1,2}$	elastance of respiratory compartment
$R_{1,2}$	resistance in respiratory model
$P_{1,2}(0)$	initial air pressure in respiratory compartment
•	element by element vector multiplication

REFERENCES

[1] Audoly, S., L. D'Angio, M. P. Saccomani, and C. Cobelli. Global identifiability of linear compartmental models–a computer algebra algorithm. *IEEE Trans. Biomed. Eng.* 45:36–47, 1998.

[2] Bates, J. H., M. Decramer, W. A. Zin, A. Harf, J. Milic-Emili, and H. K. Chang. Respiratory resistance with histamine challenge by single-breath and forced oscillation methods. *J. Appl. Physiol.* 61:873–880, 1986.

[3] Burattini, R., G. G. Knowlen, and K. B. Campbell. Two arterial effective reflecting sites may appear as one to the heart. *Circ. Res.* 86:85–99, 1991.

[4] Cappello, A., G. Gnudi, and C. Lamberti. Identification of the three-element Windkessel model incorporating a pressure-dependent compliance. *Ann. Biomed. Eng.* 23:164–177, 1995.

[5] Cobelli, C., and K. Thomaseth. Maximally informative designs in physiological modeling based on optimality-criteria gradients. In: Proceedings of the 10th IFAC World Congress on Automatic Control, edited by R. Isermann. Oxford: Pergamon, 1987, Vol. 10, pp. 231–236.

[6] Fedorov, V. V. Theory of Optimal Experiments. New York: Academic, 1972.

[7] Frank, P. M. Introduction to System Sensitivity Theory. New York: Academic, 1978.

[8] Seber, G. A. F., and C. J. Wild. Nonlinear Regression. New York: Wiley, 1989.

[9] Thomaseth, K. PANSYM: a symbolic equation generator for mathematical modeling, analysis and control of metabolic and pharmacokinetic systems. *Comput. Methods Programs Biomed.* 42:99–112, 1994.

[10] Thomaseth K. Modeling and analysis of physiological systems with MATLAB: Software development for Macintosh computer. In: Modeling and Control in Biomedical Systems, edited by B. Patterson. Oxford: Pergamon, 1994, pp. 408–409.

[11] Thomaseth, K. Analysis of errors due to assigned model constants in pharmacokinetic calculations based on functional optimisation. *Int. J. Clin. Pharmacol. Ther.* 33:555–559, 1995.

[12] Thomaseth, K. and C. Cobelli. Parameter information content during model identification experiments. In: Modeling and Control in Biomedical Systems, edited by D. A. Linkens, and E. Carson. Oxford: Pergamon, 1997, pp. 107–112.

[13] Westerhof, N., G. Elzinga, and C. G. van den Bos. Influence of central and peripheral changes on the hydraulic input impedance of the systemic arterial tree. *Med. Biol. Eng.* 11:710–723, 1973.